



Cite this: *Phys. Chem. Chem. Phys.*,
2017, **19**, 4125

Engineering magnetic anisotropy and magnetization switching in multilayers by strain

Kun Tao,^{*ab} Pengfei Liu,^a Qing Guo,^a Liya Shen,^c Desheng Xue,^a O. P. Polyakov^{bd}
and V. S. Stepanyuk^b

The effect of the strain on the magnetic properties of metallic multilayers has been investigated by *ab initio* studies. Our results indicate that the magnetic anisotropy energy (MAE) of an Fe(001) surface can be drastically enhanced by capping with 5d elements. By choosing Ir–Fe multilayers as a model system, we demonstrate that the MAE which depends on the composition and the structure of the multilayers can be tuned in a large range by strain. Furthermore, our results show that not only the amplitude of the MAE but also the easy axis of Pt–Fe multilayers can be engineered by strain. Magnetization switching by strain is also investigated.

Received 15th November 2016,
Accepted 5th January 2017

DOI: 10.1039/c6cp07811g

www.rsc.org/pccp

1 Introduction

Ultrathin or multilayer magnetic structures, one of the best examples of nanoscience and nanotechnology, have experienced a tremendous boost due to their applications in many fields.^{1–3} The key property of a ferromagnetic sample is the direction of its magnetization. One of the most active research topics in the field of ultrathin magnetic structures is to understand and manipulate their magnetic anisotropy (MA) which defines the stability of a spin in a defined direction. Many strategies to manipulate MA have been proposed, which mainly focus on tuning the spin-orbital coupling (SOC) in films, surfaces and interfaces.^{4–7} Alloying 3d elements together with 4d (5d) elements can greatly enhance the SOC of the system and thus results in a large MA, which can be used for high density data storage and nonvolatile spintronic devices.^{8–11} It was recently reported that the MA of ultrathin structures^{12,13} and magnetic molecules¹⁴ can also be tuned by an external electric field.

For ultrathin magnetic structures, magnetic properties such as magnetic moment, exchange interaction and anisotropy are sensitive to their structures, composition components and atomic-layer alignments.¹⁵ The strain in such systems can introduce changes in the d orbital occupations and results in a variation of the MA.^{16–18} Our understanding of the effect of the strain on the MA, however, is still incomplete. For example,

in an Fe film, the easy axis of the system changes from in-plane to out-of-plane and returns to in-plane again just by sequentially capping one monolayer Ni and Fe.^{19,20} But only a very small strain is observed in the experiment.¹⁹ Understanding and controlling the MA in metallic multilayers still presents one of the challenges in nanomagnetism today.

In this work, we demonstrate that the MAE of 3d metal multilayers is significantly enhanced by capping with 5d elements. Furthermore, we show that the amplitude of the MAE and the easy axis of the magnetization of magnetic multilayers can be manipulated by strain. The effect of the strain on magnetization switching is revealed.

2 Calculation methods

Our calculations are based on projector augmented wave (PAW) potentials²¹ as implemented in the Vienna *Ab initio* Simulation Package (VASP)^{22,23} and the local spin density approximation (LSDA). The generalized gradient approximation (GGA) has also been employed to check LSDA results; both of them gave the same trend with an MA variation of less than 4%. The basis set contained plane waves with a kinetic energy cutoff of 500 eV and the total energy was converged to 10^{−7} eV. A dense *k*-point mesh of 21 × 21 × 1 was used to obtain a more accurate magnetic anisotropy energy. We have used a supercell approach in which the layers in the slabs are initially interspaced by an Fe bulk interlayer distance of 1.375 Å, obtained from the calculated lattice constant of bcc Fe $a_0 = 2.75$ Å. Later on, all geometries were optimized without any symmetry constraint until all residual forces on each atom were less than 0.01 eV Å^{−1}. Such multilayer models have been adopted by many DFT calculations.^{9,12,13,15} As an example, the multilayer model for the Ir/Fe(2)/Ir/Fe(100)

^a Key Lab for Magnetism and Magnetic Materials of Ministry of Education, Lanzhou University, Lanzhou 730000, People's Republic of China.
E-mail: taokun@lzu.edu.cn

^b Max-Planck-Institute of Microstructure Physics, Halle, Germany

^c School of Physics Science and Technology, Lanzhou University, Lanzhou 730000, China

^d Physics Department, M.V. Lomonosov Moscow State University, Leninskie Gory, 119991 Moscow, Russia

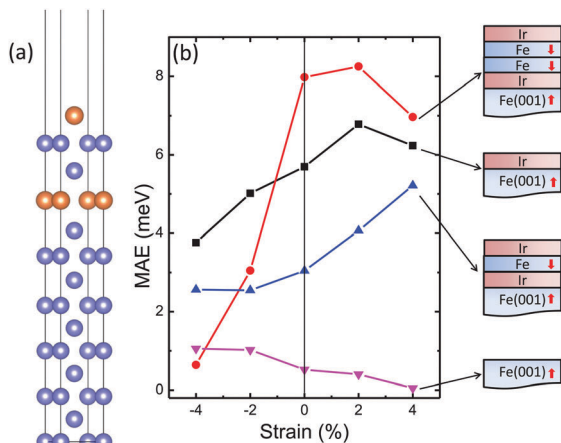


Fig. 1 (a) Multilayer model of the Ir/Fe(2)/Ir/Fe(100) system, with yellow and blue balls for Ir and Fe atoms, respectively. (b) MAE as a function of the strain ε for various Ir–Fe systems. MAE is defined as the total energy difference of the system when the spin direction of the system rotates from in-plane to out-of-plane. Vertical arrows in the figure stand for an out-of-plane axis of magnetization.

system is plotted in Fig. 1(a). The strain ε is defined as $\varepsilon = (a - a_0)/a_0 \times 100\%$, with $a_0 = 2.75 \text{ \AA}$ for bcc Fe and a being the lattice constant without and with strain, respectively. For relaxation, under strains, the in-plane x and y lattice parameters are fixed at given strain values, with the z lattice parameter relaxed and optimized with atomic coordinates. The Ir–Fe and Pt–Fe multilayers are supported by a ten-layer Fe(001) surface, which may have different spin configurations. The most energy favorable spin configuration for each system is obtained by comparing the total energy of the system with all possible spin alignments. The ground state of the system is that in which the spin direction of the Fe monolayer or bilayers sandwiched between two Ir(Pt) monolayers is perpendicular and anti-parallel to that of the Fe(001) substrate, schematically plotted in Fig. 1 and Fig. 2, respectively. The out-of-plane antiparallel spin configuration is robust for all Ir–Fe and Pt–Fe systems under any strains, except for the

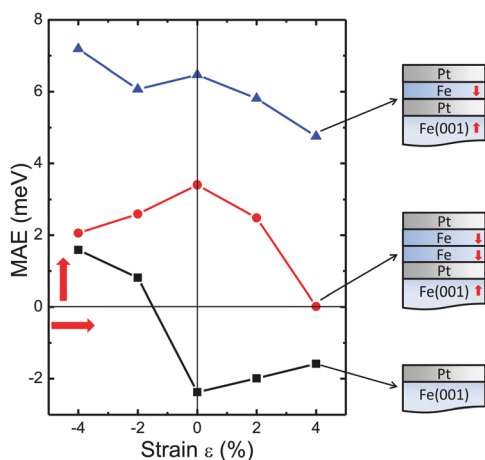


Fig. 2 MAE as a function of the strain ε for various Fe–Pt systems. Vertical (horizontal) arrows in the figure stand for an out-of-plane (in-plane) axis of magnetization.

Pt/Fe(001) system in which the spin direction changes from out-of-plane to in-plane as strain increases from the negative to positive value. Spin–orbit coupling (SOC) with a fully relativistic effect was included in all calculations. The MAE is defined as the total energy difference of the system as its spin direction rotates from parallel to perpendicular to the surface, *i.e.* $E[100] - E[001]$.

The Landau–Lifshitz–Gilbert (LLG) equation is used to study the time evolution of the magnetization. Although this phenomenological equation was used to describe the macroscopic magnetic system, it is also useful for analyzing the atomic spin dynamics after some modifications.^{24–31} We denote \mathbf{S}_i as the unit vector of the i -th atom with a magnetic moment μ_s ($\mathbf{S}_i \equiv \mu_s/|\mu_s|$). Then the magnetization dynamics can be described by the LLG equation:

$$\frac{\partial \mathbf{S}_i}{\partial t} = -\gamma \mathbf{S}_i \times \mathbf{H}_{\text{eff}}^i + \frac{\alpha}{\mu_s} \mathbf{S}_i \times \frac{\partial \mathbf{S}_i}{\partial t} \quad (1)$$

where γ – gyromagnetic ratio, α – damping parameter, and $\mathbf{H}_{\text{eff}}^i$ – effective magnetic field acting on the magnetic moment of the i -th atom. $\mathbf{H}_{\text{eff}}^i$ is determined using the exchange interactions, external magnetic field \mathbf{H} and the magnetic anisotropy:

$$\mathbf{H}_{\text{eff}}^i = \frac{\partial}{\partial \mathbf{S}_i} \left[\sum_{j(j \neq i)} \frac{J_{ij}}{\mu_s} \mathbf{S}_i \mathbf{S}_j + \mathbf{S}_i \mathbf{H} + \frac{K_i}{\mu_s} (\mathbf{S}_i \mathbf{e}_a)^2 \right], \quad (2)$$

where J_{ij} – the exchange interaction between the i -th and j -th atoms ($J_{ij} < 0$ for anti-ferromagnetic and $J_{ij} > 0$ for ferromagnetic), K_i – anisotropy energy of the i -th atom, and \mathbf{e}_a denotes the direction of the easy axis. A home-made code was used in our calculations. The values of magnetic moments, the exchange interaction and the MAE are obtained from our DFT calculations.

3 Results and discussion

The effect of the strain on the MAE in the Fe based multilayers is investigated for several capping configurations. First, a ten-layer Fe surface under zero strain has the MAE of about 0.5 meV, which is about several ten times larger than that of the bulk. The MAE of the Fe(001) surface presents a strong dependence on the strain, as plotted in Fig. 1(b). The MAE increases two times to 1.0 meV with a negative strain $\varepsilon = -4\%$, but it decreases 10 times to 0.05 meV at a positive strain $\varepsilon = +4\%$. The out-of-plane magnetization is preserved under all strains. Although the MAE of the Fe thin film can be strongly enhanced by the strain, its value is still much smaller than that of the 3d–5d combined system.⁸

In order to tune the MAE of the Fe thin film, an Ir monolayer is deposited onto the Fe(001) substrate. The MAE of the Ir/Fe(001) bilayer under zero strain ($\varepsilon = 0$) increases 10 times up to 5.7 meV, which is due to the strong spin–orbital coupling between the Ir monolayer and the top Fe layer of the substrate. It further increases by 20% to 6.8 meV under the positive strain of +2%.

By capping one additional Fe monolayer and one Ir monolayer onto the Ir/Fe(001) surface forming an Ir/Fe(1)/Ir/Fe(001) system, the MAE of such a system, however, decreases to 3.0 meV under zero strain $\varepsilon = 0$. It increases to 5.2 meV with a positive

strain of 4%, which is still smaller than that of the Ir/Fe(001) system. To check the structural sensitivity of the MAE, the Fe bilayer is sandwiched between two Ir monolayers forming an Ir/Fe(2)/Ir/Fe(001) system. The MAE of the system under zero strain undergoes a great enhancement to 8.0 meV, but it decreases linearly to 0.6 meV with a negative strain of -4% .

In Ir/Fe(1)/Ir/Fe(001) and Ir/Fe(2)/Ir/Fe(001) systems, when one or two Fe layers are sandwiched between two Ir monolayers, however, their spin directions are out-of-plane and antiparallel to those in the substrate. Since Fe and Ir have different lattice constants, it will result in different relaxation behavior and magnetic orders under external strains.^{32,33} The c/a ratio, with a and c being the in-plane lattice constant and the vertical distance between two Fe monolayers at both sides of the Ir monolayer at a given strain, respectively, under different strains has been carefully checked. After full relaxation, strong tetragonal distortions have been observed. In Ir/Fe(1)/Ir/Fe(001), the c/a ratio decreases from 1.34 to 1.11 as the strain expands from -4% to $+4\%$, and the c/a ratio changes from 1.32 to 1.08 for Ir/Fe(2)/Ir/Fe(001). To shed further light on the effect of the relaxation on the magnetic order, in both Ir/Fe(1)/Ir/Fe(001) and Ir/Fe(2)/Ir/Fe(001) configurations, all layers are fixed at their ideal positions of the bulk Fe, which correspond to $c/a = 1$. It was found that the parallel spin alignment for Fe layers at both sides of the Ir monolayer is more energetically favorable.

Now, we turn to another example of the effect of the strain on MAE. It is well known that materials with the Fe–Pt composition have high MAE and used for high density data storage.^{34–36} We calculated the effect of the strain on the MAE in Fe–Pt multilayers, as shown in Fig. 2. Under zero strain, the MAE of the Pt/Fe(001) system is about 2.4 meV, which enhances five times compared to that of the pure Fe(001) surface but two times smaller than that of the Ir/Fe(001) (Fig. 1(b)). More interesting is that the magnetization axis of the system is reoriented to be in-plane, while the easy axis of the Fe(001) substrate and the Fe–Ir multilayer system is out-of-plane. The MAE of the system linearly decreases to 1.6 meV as strain ε expands to $+4\%$ and the in-plane magnetization is preserved. The MAE decreases to 1.6 meV at a negative strain of -4% , but the easy axis of the system rotates out-of-plane.

As for the Pt/Fe(1)/Pt/Fe(001) system, the MAE strongly increases to 6.5 meV under zero strain and it linearly decreases to 4.7 meV with a positive strain of $+4\%$. The out-of-plane easy axis is preserved for all strains. The MAE decreases to 3.4 meV under zero strain for the Pt/Fe(2)/Pt/Fe(001) system, which is smaller than that of the Pt/Fe(1)/Pt/Fe(001) system. And it even further decreases to about 0 meV at a positive strain of $+4\%$. With an even larger positive strain, the easy axis may rotate in-plane.

The physics behind the MAE dependence on the strain in multilayers can be understood using the second-order perturbation approach³⁷

$$\text{MAE} \sim \xi^2 \sum_{o,u} \frac{|\langle \psi_u^\dagger | L_z | \psi_o^\dagger \rangle|^2 - |\langle \psi_u^\dagger | L_x | \psi_o^\dagger \rangle|^2}{\varepsilon_u^\dagger - \varepsilon_o^\dagger} \quad (3)$$

where the ξ parameter is an average of the spin orbital coupling coefficients, $\{\psi_u^\dagger, \psi_o^\dagger\}$ stand for the unoccupied (occupied) minority

spin-states and $\{L_x, L_z\}$ are the angular momentum operators, respectively. Since the majority part of the Fe d band is fully occupied, so the SOC between states of opposite spin can be ignored, the main changes in MAE can be attributed to the interaction between states in the minority d band.

We first start our discussion by analyzing Fe–Ir multilayers and choosing Ir/Fe(1)/Ir/Fe(001) as a representative system. Upon analysing the SOC matrix elements, one can find that the minority $d_{x^2-y^2}$ orbital of the Fe which couples with the minority d_{xy} orbital of the Fe through the L_z operator $\langle d_{x^2-y^2} | L_z | d_{xy} \rangle$ gives the largest contribution to the MAE from the first term in eqn (3), which prefers an out-of-plane magnetization. The dependence of the MA on the strain can be qualitatively inferred from the PDOS, which provides direct information about the local structure, particularly for the MA behavior. It can be seen from Fig. 3 that with negative strains the population of the d_{xy} orbital of the Fe slightly increases while that of the $d_{x^2-y^2}$ orbital reduces largely near the Fermi level, decreasing strengths of the SOC between them and resulting in a slight decrease in MA. On the other hand, with positive strains, the $d_{x^2-y^2}$ orbital undergoes a fast increase near the Fermi level and, thus, enhances the coupling $\langle d_{x^2-y^2} | L_z | d_{xy} \rangle$, leading to a linear increase in the out-of-plane MA. Similar analysis can also be applied to other Fe–Ir systems, such as Ir/Fe(100) and Ir/Fe(2)/Ir/Fe(100) systems.

The magnetic behavior of Fe–Pt multilayers is quite different from that of Fe–Ir multilayers. For example, as strain $\varepsilon = 0$, the easy axis of the Pt/Fe(001) system is in-plane and to be out-of-plane for Pt/Fe(1)/Pt/Fe(001) and Pt/Fe(2)/Pt/Fe(001) systems, while those are always out-of-plane for all Fe–Ir multilayers. We choose Pt/Fe(001) and Pt/Fe(1)/Pt/Fe(001) systems as representative systems and analyze their magnetic properties under different strains. Starting from the Pt/Fe(001) system, we plot the d-resolved DOS of the Fe in Fig. 4. The coupling between d_{xz} and d_{xy} orbitals through the L_x operator $\langle d_{xz} | L_x | d_{xy} \rangle$ gives the main contribution to the in-plane anisotropy through the second

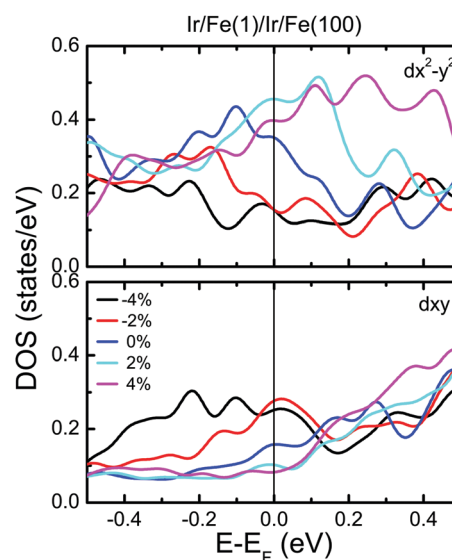


Fig. 3 Projected minority d-orbital density of states (DOS) for the Fe layer sandwiched between two Ir layers in Ir/Fe(1)/Pt/Fe(001) under different strains.

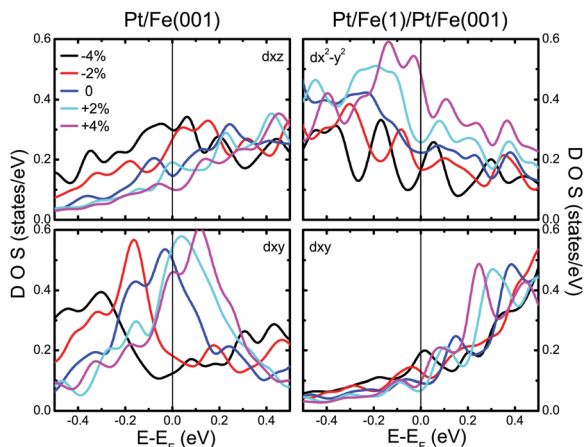


Fig. 4 Projected minority d-orbital density of states (DOS) for Fe–Pt systems. Left panel: Decomposed d-orbitals for the top Fe layer of the substrate in Pt/Fe(001). Right panel: Decomposed d-orbitals for the Fe layer sandwiched between two Ir layers in Pt/Fe(1)/Pt/Fe(001).

term in eqn (3). Under negative strains, the d_{xy} orbitals decrease significantly near the Fermi level, reducing the spin–orbital coupling between them and, therefore, giving rise to an out-of-plane magnetization. With positive strains, the d_{xy} orbitals increase near the Fermi level and the d_{xz} orbitals slightly decrease near the Fermi level, resulting in a slightly decreased MA, as shown in Fig. 2. For the Pt/Fe(1)/Pt/Fe(001) system, the coupling $\langle d_{x^2-y^2} | L_z | d_{xy} \rangle$ gives significant contribution to MA, which favours an out-of-plane magnetization. As strain increases from negative to positive values, the decreased $d_{x^2-y^2}$ orbital occupation near the Fermi level results in a partial cancellation of the slightly enhanced d_{xy} orbital, resulting in decreasing coupling between them through the L_z operator $\langle d_{x^2-y^2} | L_z | d_{xy} \rangle$, leading to an out-of-plane magnetization.

Finally, we show that magnetization dynamics in multilayers can be tailored by strains. We perform magnetization switching calculations by using the Landau–Lifshitz–Gilbert equation similar to that reported in our previous works.^{25,38} The Runge–Kutta fourth-order method with a time step of $t = 10^{-18}$ s and a damping parameter $\alpha = 0.01$ (which is a typical value in experiments³⁹) has been applied to all calculations. *Ab initio* calculated magnetic moments and MAE are used in all calculations. In the case of the Ir/Fe(2)/Ir/Fe(001) system, the macrospin approximation,⁴⁰ *i.e.* all atomistic spins within the Fe bilayer between two Ir monolayers are assumed to corotate, is applied to all spin dynamics calculations. The exchange interactions between the Fe bilayer and the Fe(001) substrate are -1.27 meV for -4% strain and -1.63 meV for 0% strain.

To achieve the magnetization switching, two scenarios have been proposed: one is that two constant magnetic fields are exerted on systems, which have orientation along/perpendicular to their easy axis (denoted as H_{easy} and H), respectively. The second one applies only short rectangular magnetic pulses to systems, which are perpendicular to their easy axis. Choosing the Ir/Fe(2)/Ir/Fe(001) system as a typical example (Fig. 5(a)), it can be found that under the -4% strain the minimum value of the switching magnetic field is strongly reduced from 32 T to 4 T

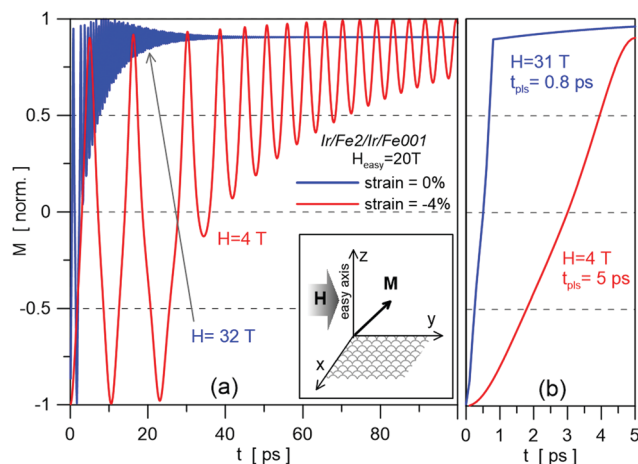


Fig. 5 Magnetization switching of the top Fe monolayers in the Ir/Fe(2)/Ir/Fe(001) system by constant magnetic fields (a) and by short magnetic pulses (b). t_{puls} denotes the pulse duration time. Directions of the easy axis of the system and the magnetic field (pulse) that perpendicular to the easy axis are plotted in the inset of (a).

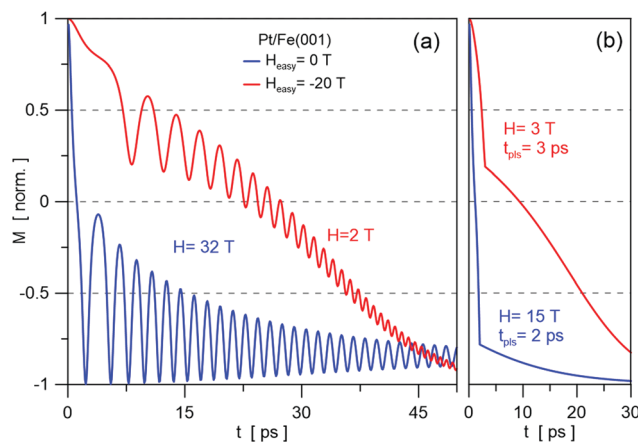


Fig. 6 Magnetization switching for the Pt/Fe(001) system by (a) constant magnetic fields and (b) short magnetic pulse.

in comparison with that under zero strain. The switching time, however, increases from 25 ps to 100 ps. The switching time can be drastically reduced by applying short magnetic pulses, as shown in Fig. 5(b). The external strain can be used to significantly reduce the magnitude of the magnetic pulses needed for switching.

A similar effect of the strain can also be found in the Pt/Fe(001) system (Fig. 6(a)). As was shown before that under the strain of -4% its easy axis is out-of-plane. Here, we can detect that magnetization switching occurs at $H = 32$ T with $H_{\text{easy}} = 0$ and $H = 2$ T with $H_{\text{easy}} = -20$ T (Fig. 6(a)). The switching time is about 50 ps for both cases. Using short magnetic pulses one can significantly reduce the strength of the magnetic field and the switching time as shown in Fig. 6(b).

4 Conclusions

In summary, we have studied the effect of the strain on the MAE in magnetic multilayers. The MAE of such systems is sensitive

to their structures and the 5d element capping. Furthermore, we demonstrated that the magnitude of the MAE of such systems can be manipulated in a large range by external strains, which can be qualitatively explained by the second-order perturbation theory. Moreover, in comparison with Ir–Fe multilayers, we prove that both the amplitude of the MAE and the magnetization axis of Pt–Fe multilayers can be tuned by strains. The significant influence of strain on the magnetization dynamics is revealed. In experiments, such strains can be achieved, for example by the magnetoelectric effect. It has been reported that in ferroelectric/ferromagnetic junctions the MA of such heterostructures can be manipulated by the interfacial strains.^{41,42} Here, we have presented a theoretical prediction of tuning the magnetic properties of multilayers by strains, which could be used to design new functional spintronic devices.

Acknowledgements

This work is supported by the National Natural Science Foundation of China (Grant No. NSFC-11274146), the National Basic Research Program of China (Grant No. 2012CB933101), the Fundamental Research Funds for the Central Universities (Grant No. Lzujbky-2014-27), and the DFG project “Structure and magnetism of cluster ensembles on metal surfaces: microscopic theory of the fundamental interactions” (PA 429/5). Part of the work was carried out at National Supercomputer Center in Tianjin, and the calculations were performed on TianHe-1 (A).

References

- M. N. Baibich, J. M. Broto, A. Fert, F. N. Van Dau, F. Petroff, P. Etienne, G. Creuzet, A. Friederich and J. Chazelas, *Phys. Rev. Lett.*, 1988, **61**, 2472–2475.
- G. Binasch, P. Grünberg, F. Saurenbach and W. Zinn, *Phys. Rev. B: Condens. Matter Mater. Phys.*, 1989, **39**, 4828–4830.
- S. S. P. Parkin, C. Kaiser, A. Panchula, P. M. Rice, B. Hughes, M. Samant and S.-H. Yang, *Nat. Mater.*, 2004, **3**, 1476.
- R. Wu and A. Freeman, *J. Magn. Magn. Mater.*, 1999, **200**, 498–514.
- C. F. Hirjibehedin, C.-Y. Lin, A. F. Otte, M. Ternes, C. P. Lutz, B. A. Jones and A. J. Heinrich, *Science*, 2007, **317**, 1199–1203.
- B. Bryant, A. Spinelli, J. J. T. Wagenaar, M. Gerrits and A. F. Otte, *Phys. Rev. Lett.*, 2013, **111**, 127203.
- I. G. Rau, S. Baumann, S. Rusponi, F. Donati, S. Stepanow, L. Gragnaniello, J. Dreiser, C. Piamonteze, F. Nolting, S. Gangopadhyay, O. R. Albertini, R. M. Macfarlane, C. P. Lutz, B. A. Jones, P. Gambardella, A. J. Heinrich and H. Brune, *Science*, 2014, **344**, 988–992.
- P. Gambardella, S. Rusponi, M. Veronese, S. S. Dhesi, C. Grazioli, A. Dallmeyer, I. Cabria, R. Zeller, P. H. Dederichs, K. Kern, C. Carbone and H. Brune, *Science*, 2003, **300**, 1130–1133.
- J. Dorantes-Dávila, H. Dreyssé and G. M. Pastor, *Phys. Rev. Lett.*, 2003, **91**, 197206.
- G. Moulas, A. Lehnert, S. Rusponi, J. Zablouil, C. Etz, S. Ouazi, M. Etzkorn, P. Bencok, P. Gambardella, P. Weinberger and H. Brune, *Phys. Rev. B: Condens. Matter Mater. Phys.*, 2008, **78**, 214424.
- A. Lehnert, S. Dennler, P. Błoński, S. Rusponi, M. Etzkorn, G. Moulas, P. Bencok, P. Gambardella, H. Brune and J. Hafner, *Phys. Rev. B: Condens. Matter Mater. Phys.*, 2010, **82**, 094409.
- C.-G. Duan, S. S. Jaswal and E. Y. Tsymbal, *Phys. Rev. Lett.*, 2006, **97**, 047201.
- P. Ruiz-Díaz, T. R. Dasa and V. S. Stepanyuk, *Phys. Rev. Lett.*, 2013, **110**, 267203.
- J. Hu and R. Wu, *Phys. Rev. Lett.*, 2013, **110**, 097202.
- K. Hotta, K. Nakamura, T. Akiyama, T. Ito, T. Oguchi and A. J. Freeman, *Phys. Rev. Lett.*, 2013, **110**, 267206.
- D. Sander, *J. Phys.: Condens. Matter*, 2004, **16**, R603.
- O. O. Brovko, D. I. Bazhanov, H. L. Meyerheim, D. Sander, V. S. Stepanyuk and J. Kirschner, *Surf. Sci. Rep.*, 2014, **69**, 159–195.
- P. Ravindran, A. Kjekshus, H. Fjellvåg, P. James, L. Nordström, B. Johansson and O. Eriksson, *Phys. Rev. B: Condens. Matter Mater. Phys.*, 2001, **63**, 144409.
- H. L. Meyerheim, D. Sander, R. Popescu, J. Kirschner, O. Robach and S. Ferrer, *Phys. Rev. Lett.*, 2004, **93**, 156105.
- J.-S. Lee, J. T. Sadowski, H. Jang, J.-H. Park, J.-Y. Kim, J. Hu, R. Wu and C.-C. Kao, *Phys. Rev. B: Condens. Matter Mater. Phys.*, 2011, **83**, 144420.
- P. E. Blöchl, *Phys. Rev. B: Condens. Matter Mater. Phys.*, 1994, **50**, 17953–17979.
- G. Kresse and J. Hafner, *Phys. Rev. B: Condens. Matter Mater. Phys.*, 1993, **47**, 558–561.
- G. Kresse and J. Furthmüller, *Phys. Rev. B: Condens. Matter Mater. Phys.*, 1996, **54**, 11169–11186.
- R. Wieser, V. Caciuc, C. Lazo, H. Hölscher, E. Y. Vedmedenko and R. Wiesendanger, *New J. Phys.*, 2013, **15**, 013011.
- O. P. Polyakov and V. S. Stepanyuk, *J. Phys. Chem. Lett.*, 2015, **6**, 3698–3701.
- B. Zhang, W. Wang, M. Beg, H. Fangohr and W. Kuch, *Appl. Phys. Lett.*, 2015, **106**, 102401.
- B. Skubic, J. Hellsvik, L. Nordström and O. Eriksson, *J. Phys.: Condens. Matter*, 2008, **20**, 315203.
- S. Bhattacharjee, A. Bergman, A. Taroni, J. Hellsvik, B. Sanyal and O. Eriksson, *Phys. Rev. X*, 2012, **2**, 011013.
- M. Sayad and M. Potthoff, *New J. Phys.*, 2015, **17**, 113058.
- R. F. L. Evans, W. J. Fan, P. Chureemart, T. A. Ostler, M. O. A. Ellis and R. W. Chantrell, *J. Phys.: Condens. Matter*, 2014, **26**, 103202.
- L. Rozsa, L. Udvardi and L. Szunyogh, *J. Phys.: Condens. Matter*, 2014, **26**, 216003.
- T. Burkert, O. Eriksson, P. James, S. I. Simak, B. Johansson and L. Nordström, *Phys. Rev. B: Condens. Matter Mater. Phys.*, 2004, **69**, 104426.
- R. Wu, L. Chen, A. Shick and A. Freeman, *J. Magn. Magn. Mater.*, 1998, **177**, 1216–1219.
- M. Tsujikawa and T. Oda, *Phys. Rev. Lett.*, 2009, **102**, 247203.
- T. R. Dasa, P. Ruiz-Díaz, O. O. Brovko and V. S. Stepanyuk, *Phys. Rev. B: Condens. Matter Mater. Phys.*, 2013, **88**, 104409.

- 36 J. B. Staunton, S. Ostanin, S. S. A. Razee, B. L. Gyorffy, L. Szunyogh, B. Ginatempo and E. Bruno, *Phys. Rev. Lett.*, 2004, **93**, 257204.
- 37 D.-s. Wang, R. Wu and A. J. Freeman, *Phys. Rev. B: Condens. Matter Mater. Phys.*, 1993, **47**, 14932–14947.
- 38 K. Tao, O. P. Polyakov and V. S. Stepanyuk, *Phys. Rev. B*, 2016, **93**, 161412.
- 39 A. Chudnovskiy, C. Hubner, B. Baxevanis and D. Pfannkuche, *Phys. Status Solidi B*, 2014, **251**, 123915.
- 40 S. Bhattacharjee, A. Bergman, A. Taroni, J. Hellsvik, B. Sanyal and O. Eriksson, *Phys. Rev. X*, 2012, **2**, 011013.
- 41 C. A. F. Vaz, *J. Phys.: Condens. Matter*, 2012, **24**, 333201.
- 42 J. Hu, L. Chen and C. Nan, *Adv. Mater.*, 2016, **28**, 15.